Drop Breakup in Turbulent Stirred-Tank Contactors

Part II: Relative Influence of Viscosity and Interfacial Tension

The relative influence of dispersed-phase viscosity and interfacial tension on equilibrium drop size and drop size distribution is studied for dilute suspensions by dispersing various silicone oils in water, methanol, and their solutions. Correlations for Sauter mean diameter, D_{32}, are developed in terms of system variables using the mechanistic models of Part I. Drop sizes for low to moderate viscosity dispersed phases are normally distributed in volume and can be correlated by normalization with D_{32}. Trends in the distributions are explained in terms of a parameter representing the relative resistance to breakage.

C. Y. Wang and R. V. Calabrese
Department of Chemical and Nuclear
Engineering
University of Maryland
College Park, MD 20742

SCOPE

In Part I the effect of dispersed-phase viscosity on mean equilibrium drop size and size distribution was examined for dilute liquid-liquid systems exhibiting constant interfacial tension. Moderate ($\mu_d' = 0.1$ and 0.5 Pa · s) and high ($\mu_d' = 5.$ and 10 Pa · s) viscosity dispersed phases behaved differently with respect to the dependency of mean size on system variables and the functional form of the size distribution, and were separated by a region of erratic behavior. The study was, in many respects, a survey that determined the scope of the problem and defined the relevant parameters for data correlation.

This study focuses in more detail on dilute liquid-liquid systems with low to moderate ($0.001 \le \mu_d' \le 0.5$ Pa · s) viscosity dispersed phases. The major objectives are to determine the relative contribution of interfacial tension and viscosity to drop stability, and to develop practical correlations for mean size and drop size distribution that remain valid in the limit of an inviscid dispersed phase. Additionally, an intermediate ($\mu_d' = 1$ Pa · s) viscosity oil, which exhibited erratic behavior in Part I, is examined over a range of interfa-

cial tension, σ, to gain insight into the influence of σ on the transition between moderate- and high-viscosity behavior.

The results of numerous experiments, conducted in the geometry of Part I using similar techniques, are reported for dilute dispersions of silicone oils in water, methanol, and their solutions. Since these oils exhibit about the same interfacial tension with a given continuous phase, it was possible to systematically vary viscosity and interfacial tension over the range $0.001 < \mu_d' < 1$ Pa · s and $0.001 < \sigma' < 0.045$ N/m.

The semiempirical theory of Part I is used to develop correlations for equilibrium mean drop size and a criterion for when viscous resistance to breakage can be neglected. These are in terms of two dimensionless groups containing only system variables, namely, tank Weber number, We, and viscosity group, Vi. A parameter E_R, which is a measure of the relative resistance to breakage, is defined to aid in data interpretation and the development of a correlation for equilibrium drop size distribution.

The range of variables studied includes $54 < We < 71,000$, $0.0041 < Vi < 640$, and $14,000 < Re < 83,000$. The results apply to dilute (noncoalescing) suspensions produced by six-blade Rushton turbines in baffled cylindrical tanks of standard geometry.

CONCLUSIONS AND SIGNIFICANCE

The experimental data have been analyzed, correlated with relevant system parameters, and compared to literature data for inviscid dispersed phases. The following conclusions apply for the range of variables studied.

1. At constant conditions of agitation, the relative influence of interfacial tension decreases as dispersed-phase viscosity increases. For low interfacial tension systems, surface resistance to breakage becomes negligible relative to viscous resistance at $\mu'_d \simeq$ 1 Pa · s. At high σ much larger μ_d is required to reach this limit.

2. Equilibrium drop sizes for low to moderate (0.001 $\leq \mu'_d \leq$ 0.5 Pa · s) viscosity dispersed phases are normally distributed in volume. At higher viscosity ($\mu'_d = 1$ Pa · s) deviations from normality occur but only in higher interfacial tension systems. This suggests that the transition from moderate- to high-viscosity behavior, as depicted in Part I, shifts to higher μ_d as σ decreases.

3. Drop size distributions broaden as interfacial tension and viscosity increase and as impeller speed decreases. This is consistent with an increase in the relative resistance to breakage, E_R, as defined by Eq. 9. Therefore E_R provides a measure of the broadness of the distribution. Furthermore, observations of drop breakup suggest that this broadening is consistent with a shift in the predominant breakage mechanism from bursting toward stretching.

4. Dimensionless mean drop size for low to moderate viscosity dispersed phases are well-correlated in terms of tank Weber number and viscosity group by a semitheoretical model containing two adjustable geometric parameters. The model reduces to the Weber number correlation of Chen and Middleman (1967) in the limit of an inviscid dispersed phase ($Vi = 0$), and provides a criterion by which the relative influence of viscosity and interfacial tension can be assessed. A correlation with six adjustable parameters, developed by modifying the semitheoretical model, provides an excellent fit to the data. A more easily applied three-parameter model, after Hinze (1955) and Sleicher (1962), also gives a good fit.

5. For low to moderate viscosity dispersed phases, drop size distributions can be correlated by normalization with Sauter mean diameter. The correlation for the normalized volume distribution is indistinguishable from that obtained by Chen and Middleman (1967) for inviscid drops, indicating that low- and moderate-viscosity dispersed phases behave similarly.

The correlations developed herein apply to a wide range of physical properties and operating conditions. They serve as a rational extension of accepted techniques for dilute inviscid dispersed phases in contact with a turbulent continuous phase. It would be useful to incorporate the results of other investigators into the models of this study in order to develop validated correlations for routine design purposes. This is accomplished in Part III of this paper.

Introduction

The objective of this work is to determine the relative influence of interfacial tension and dispersed-phase viscosity on equilibrium mean drop size and size distribution for dilute dispersions produced by turbulent stirred-tank contactors. The role of interfacial tension at low dispersed-phase viscosity has been considered by numerous investigators; most of these studies are summarized by Tavlarides and Stamatoudis (1981).

The extent to which dispersed-phase viscosity influences equilibrium mean drop size and drop size distribution at constant interfacial tension has been considered for dilute suspensions in Part I of this paper. A review of relevant literature is given. The liquid-liquid systems employed encompassed a broad viscosity range (0.1 $\leq \mu'_d \leq$ 10 Pa · s) and exhibited relatively high interfacial tension. Moderate ($\mu'_d = 0.1$ and 0.5 Pa · s) and high ($\mu'_d =$ 5 and 10 Pa · s) viscosity dispersed phases behaved differently with respect to the functional form of the size distribution and the manner in which mean drop size depended upon system parameters. These behaviors were separated by a transition region at intermediate ($\mu'_d = 1$ Pa · s) viscosity. A semitheoretical correlation, derived via mechanistic arguments, correlated the moderate-viscosity mean size data and provided acceptable parameters for correlation of the high-viscosity data. Certain trends in the data could be interpreted by reference to observations of the breakup mechanism for low to moderate viscosity drops. Similar observations are required to properly interpret the intermediate to high-viscosity results.

The results of Part I indicate that considerable effort is required to systematically categorize the relative contributions of interfacial tension and dispersed-phase viscosity to drop stability. As a result this study is limited to the range 0.001 $\leq \mu'_d \leq$ 1 Pa · s for several reasons. Low to moderate viscosity data are required over a wide range of interfacial tension to define the region encompassing negligible to finite viscous resistance to breakup. The semiempirical theory of Part I appears valid in this region, allowing development of correlations of practical utility. Furthermore, the mechanistic arguments on which the theory is based can be used to interpret the data. Drop size distributions display similar behavior so it may be possible to correlate them by a single expression. Observations of the breakup

mechanism are available to aid in data interpretation. Arguments presented in Part I suggest that the location of the transition between moderate- and high-viscosity behavior may be a function of interfacial tension. It is convenient to concurrently investigate this hypothesis.

As discussed above, mean drop sizes for low to moderate viscosity dispersed phases may be correlated by Eq. 18 of Part I with N_{Vi} given by Eq. 19. It is useful to recast these so that the relevant correlating variables are based only upon system parameters. This is accomplished by combining Eqs. 1, 11, 18, and 19 of Part I to obtain

$$\frac{D_{32}}{L} = A \ We^{-3/5} \left[1 + B_1 \ Vi \left(\frac{D_{32}}{L} \right)^{1/3} \right]^{3/5} \qquad (1)$$

$$We = \frac{\rho_c N^2 L^3}{\sigma}; \quad Vi = \frac{\mu_d N L}{\sigma} \left(\frac{\rho_c}{\rho_d} \right)^{1/2} \qquad (2)$$

Vi is a tank viscosity group or capillary number representing the ratio of dispersed-phase viscous to surface forces. The limits $Vi \rightarrow 0$ and $Vi \rightarrow \infty$ correspond to negligible viscous and surface resistance to breakage, respectively. Furthermore, $N_{Vi} \sim Vi(D_{32}/L)^{1/3}$. It should be noted that Eq. 1 can also be derived by casting the mechanistic arguments of Part I within the framework of the transitional breakage probability model of Narsimhan et al. (1979). The details are given by Wang (1984).

In the limit of negligible viscous resistance to breakage, Eq. 1 yields the well-known Weber number correlation

$$\frac{D_{32}}{L} = A \ We^{-3/5} \quad (Vi \rightarrow 0) \qquad (3)$$

In the limit of negligible surface resistance, Eq. 1 yields

$$\frac{D_{32}}{L} = A^{5/4} B_1^{3/4} \left(\frac{\rho_c}{\rho_d} \right)^{3/8} \left(\frac{\mu_d}{\mu_c} \right)^{3/4} Re^{-3/4} \quad (Vi \rightarrow \infty) \qquad (4)$$

$$Re = \rho_c N L^2 / \mu_c \qquad (5)$$

The viscosity group Vi provides a qualitative measure of the relative importance of dispersed-phase viscosity and interfacial tension. A quantative estimate can be obtained from Eq. 1. For the limit $Vi \rightarrow 0$, Eq. 3 can be substituted into Eq. 1 to show that surface forces predominate over viscous forces when

$$Vi \ We^{-1/5} \ll A^{-1/3} \ B_1^{-1} \qquad (6)$$

Equation 1 is an implicit relationship for Sauter mean diameter. Although its solution is not difficult, since it has only one positive real root, an explicit correlation for D_{32} is desirable from a practical viewpoint. Consider the relationship proposed by Hinze (1955), given by Eqs. 3 and 4 of Part I. It was argued there that N'_{Vi} should be replaced by N_{Vi}. The data of Chen and Middleman (1967) and of Part I reveal that for low to moderate viscosity dispersed phases, $(D_{32}/L)^{1/3}$ varies by about a factor of three, while Vi varies over more than four orders of magnitude. Since D_{32}/L increases with Vi, it is reasonable to approximate N_{Vi} by Vi and to replace $\psi(N'_{Vi})$ in Hinze's proposal by $\psi(Vi)$.

Then Eqs. 3, 4, 8–11, and 17 of Part I can be combined to yield

$$\frac{D_{32}}{L} = A \ We^{-3/5} [1 + \psi(Vi)]^{3/5} \qquad (7)$$

Sleicher (1962) argued on physical grounds that N'_{Vi} should be replaced by a viscosity group such as Vi to correlate drop breakup data for turbulent pipe flow. Except for density ratio, Vi and Eq. 7 are the stirred tank equivalents of Sleicher's viscosity group and correlation, respectively. For most liquid-liquid systems, $\sqrt{\rho_c/\rho_d}$ is of order unity. Sleicher's data and those of Part I suggest that $\psi(Vi)$ can be approximated by

$$\psi(Vi) = B_2 Vi^c \qquad (8)$$

It is argued in Part I that a useful parameter for the interpretation of drop size distribution data is the ratio of cohesive to disruptive energy acting on a drop. An expression for this quantity can be obtained for low to moderate viscosity dispersed phases by letting $R = \epsilon/\bar{\epsilon} =$ ratio of local to mean energy dissipation rate. Then Eqs. 5–9, 11, and 12 of Part I can be combined to yield

$$E_R = \frac{E_s + E_v}{E_T}$$

$$= \frac{\alpha_1 \sigma}{\rho_c (R \ N^3 L^2)^{2/3} D^{5/3}} + \frac{\alpha_2 \ \mu_d}{(\rho_c \rho_d)^{1/2} (R \ N^3 L^2)^{1/3} D^{4/3}} \qquad (9)$$

E_R represents a relative resistance to breakage. The terms on the righthand side of Eq. 9 represent the surface and viscous contributions, respectively.

Experiments and Data Reduction

In order to determine the relative importance of interfacial tension and dispersed-phase viscosity, silicone oils (Dow Corning 200 Fluids) of nine viscosity grades were dispersed in distilled water, methanol, and three aqueous methanol solutions. Silicone oils exhibit high interfacial tension with water and very low interfacial tension with methanol. All grades have about the same interfacial tension with a particular continuous phase. It was therefore possible to systematically vary σ and μ_d over wide ranges. A matrix of nominal dispersed phase viscosities and interfacial tensions was developed to facilitate discussion.

Methanol is slightly soluble in silicone oil. This solubility affected physical properties so all experiments were conducted (at 25°C) between mutually saturated phases. Viscosities were measured with Cannon-Fenske viscometers and densities were measured by a volumetric technique. Interfacial tensions were measured via a du Noüy ring technique by placing the sample vessel on a slowly moving stage and suspending the ring from a Cahn-RH Electrobalance.

Dispersed-phase viscosities and interfacial tensions are given in Tables 1 and 2, respectively. For silicone oil-water systems, interfacial tensions varied with oil grade and are about 20% higher than those reported in Table 1 of Part I. This rather alarming result was at first attributed to measurement error. The du Noüy ring apparatus used here was built to mimic the commercial instrument used in Part 1. A thorough investigation of experimental technique and instrument accuracy could not

Table 1.   Viscosity of Dispersed Phase (Pa·s) Saturated with Continuous Phase, 25°C

Dispersed Phase, Silicone Oil — Nominal Viscosity μ'_d, Pa·s	Continuous Phase, Aqueous Methanol Solutions (Nominal Interfacial Tension, σ', N/m)				
	Water $\sigma' = 0.045$	25% MeOH-H$_2$O* $\sigma' = 0.023$	50% MeOH-H$_2$O* $\sigma' = 0.015$	75% MeOH-H$_2$O* $\sigma' = 0.007$	Methanol $\sigma' = 0.001$
0.001	0.00085	0.00081	0.00081	0.00082	—
0.005	0.00428	0.00410	—	—	—
0.01	0.00963	0.00950	—	—	0.00949
0.02	0.0182	0.0174	0.0175	0.0174	0.0174
0.05	0.0424	0.0406	—	—	0.0406
0.1	0.0908	0.0876	0.0873	0.0875	0.0874
0.2	0.185	0.178	—	—	0.178
0.5	0.459	0.406	0.403	0.403	0.403
1.0	1.040	1.005	1.005	0.998	0.990

*Volume percent of methanol in water.

resolve the large difference. When the data obtained here were compared to those of Part 1 for the corresponding liquid-liquid pairs, it was found that mean drop sizes for the former were always larger. It was therefore concluded that the interfacial tension measurements were correct. The oils used here were purchased at a later time and from a different distributor than those of Part I. One should measure properties of these oils for each batch acquired. Densities of both phases and continuous phase viscosities are given in Table 3. These quantities varied by less than 0.2% when saturated with the other phase, so only average values are given. Exact values for each liquid-liquid pair are reported by Wang (1984).

The experiments were conducted in the same apparatus as in Part I. However, only the three smallest of the four tanks were used. The same experimental techniques were employed except that the dispersed-phase volume fraction was limited to $\phi \leq 0.002$ and at least 2 h was allowed to achieved equilibrium in all experiments.

The photographic system was the same as in Part I except that a 105 mm Nikkor f:2.5 lens was used to achieve higher magnification and the camera was equipped with a motor drive. Lighting requirements were such that the flash could keep pace with the motor drive (5 frames/s). Sufficient data to determine the drop size distribution could be acquired in less than 2 s,

insuring that the sampling time was of the order of or less than the tank recirculation time (Brown and Pitt, 1970).

Experiments were performed at two or three impeller speeds in each tank for each dispersed-phase oil with three of the continuous phases (H$_2$O; 25% MeOH-H$_2$O; MeOH). An exception was the $\mu'_d = 0.001$ and 0.005 Pa·s oils dispersed in methanol. No data were acquired for these systems since drop sizes were below the resolution of the photographic technique. Selected runs were made with the other two continuous phases. The range of variables covered by the 170 experiments includes $1.4 < N < 4.7$ rps, $14,000 < Re < 83,000$, $54 < We < 71,000$, and $0.0041 < Vi < 640$. The details of the experimental program are reported by Wang (1984).

Drop sizes were determined using a semiautomated digitizing machine. A 35 mm filmstrip projector was used to project the negative onto a screen. By manually moving an arm with crosshairs, the coordinates of two diametrically opposed points on each drop's surface were sent to a computer for processing. The mean drop size and drop size distribution were determined from at least 500 counts of drop diameter.

The Sauter mean diameter was calculated from

$$D_{32} = \sum_{i=1}^{n_T} D_i^3 \Big/ \sum_{i=1}^{n_T} D_i^2 \qquad (10)$$

Table 2.   Interfacial Tension (N/m) Between Mutually Saturated Phases, 25°C

Dispersed Phase, Silicone Oil — Nominal Viscosity μ'_d, Pa·s	Continuous Phase, Aqueous Methanol Solutions Nominal Interfacial Tension, σ', N/m				
	Water $\sigma' = 0.045$	25% MeOH-H$_2$O* $\sigma' = 0.023$	50% MeOH-H$_2$O* $\sigma' = 0.015$	75% MeOH-H$_2$O* $\sigma' = 0.007$	Methanol $\sigma' = 0.001$
0.001	0.0432	0.0214	0.0168	0.00905	—
0.005	0.0433	0.0243	—	—	—
0.01	0.0467	0.0240	—	—	0.00157
0.02	0.0463	0.0233	0.0150	0.00705	0.00126
0.05	0.0462	0.0236	—	—	0.00082
0.1	0.0467	0.0226	0.0146	0.00660	0.00059
0.2	0.0470	0.0222	—	—	0.00033
0.5	0.0433	0.0223	0.0143	0.00600	0.00021
1.0	0.0451	0.0222	0.0152	0.00705	0.00139

*Volume percent of methanol in water.

Table 3. Miscellaneous Physical Properties, 25°C

Density of Dispersed Phase, Silicone Oils*

μ'_d, Pa · s	0.001	0.005	0.01	0.02	0.05	0.1	0.2	0.5	1.0
ρ_d, kg/m³	834	929	946	963	963	985	986	973	968

Physical Properties of Continuous Phase**

Aqueous Methanol Solution† σ', N/m	Viscosity μ_c, Pa · s	Density ρ_c, kg/m³
Water, $\sigma' = 0.045$	0.00089	997
25% MeOH-H₂O, $\sigma' = 0.023$	0.00080	943
50% MeOH-H₂O, $\sigma' = 0.015$	0.00071	881
75% MeOH-H₂O, $\sigma' = 0.007$	0.00062	838
Methanol, $\sigma' = 0.001$	0.00055	792

*Average value for saturation with all continuous phases
**Average value for saturation with all dispersed phases
†Volume percent of methanol (MeOH) in water (H₂O)

The cumulative volume frequency was calculated from

$$F_v(D_i) = \sum_{J=1}^{i} D_J^3 \bigg/ \sum_{J=1}^{n_T} D_J^3 \qquad (11)$$

Other mean diameters and distributions were also obtained and are reported by Wang (1984).

Results and Discussion

Figure 1 gives Sauter mean diameter vs. dispersed-phase viscosity for oil-water suspensions produced in the 0.2 m tank at three impeller speeds. Near the inviscid limit, D_{32} increases slowly with μ_d. At higher viscosities the increase is more rapid. For a given μ_d, D_{32} increases as N decreases, as expected. Figure 2 is a plot of D_{32} vs. μ_d at constant power input with nominal interfacial tension as a parameter. At low viscosity, drop sizes vary by more than a factor of six over the σ range investigated, while for the highest μ_d they only vary by a factor of two. The influence of interfacial tension becomes less pronounced as μ_d increases. For the low σ systems, the slope of the curves approaches ¾ at large μ_d. This is just the μ_d dependency predicted by Eq. 4 for the limit of negligible surface resistance to breakage. It appears that this limit is at hand in these systems. The high σ data of Part I show finite surface resistance at much higher μ_d.
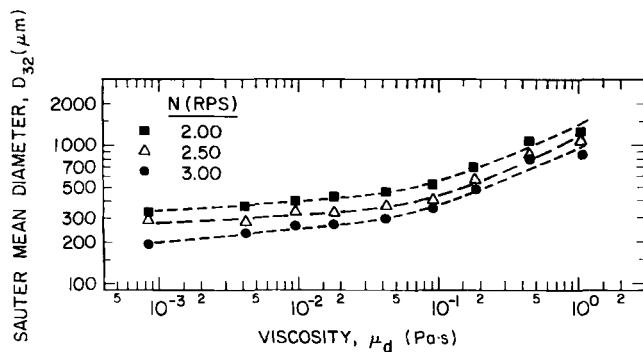

Figure 1. Effect of dispersed-phase viscosity and impeller speed on Sauter mean diameter for silicone oils dispersed in water. $\sigma' = 0.045$ N/m; $T' = 0.2$ m.
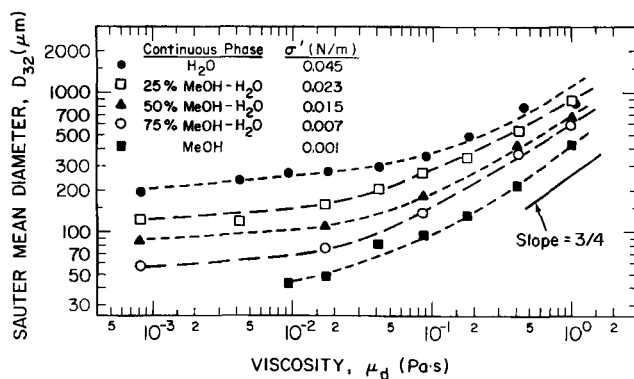

Figure 2. Relative influence of dispersed-phase viscosity and interfacial tension on Sauter mean diameter for constant conditions of agitation. $N = 3.00$ rps; $T' = 0.2$ m.

Figure 3 presents cumulative volume frequencies, on normal probability coordinates, as a function of μ_d for oils dispersed in water in the 0.15 m tank at 4.67 rps. The data are consistent with those of Part I in that the distribution broadens as μ_d increases. Except for the 1 Pa · s oil, size distributions can be represented by a straight line and are therefore about normally distributed in volume. This does not conflict with the results of Part I since many of the low to moderate viscosity data could also be approximated by a normal distribution in number. The data of Part I show that as μ_d increases, the size of the smallest drops decreases while their number increases. This is also the case here. The smallest drops contribute negligibly to dispersed-phase volume, so loss of this information is of little practical consequence, particularly since it allows all low to moderate viscosity distributions to be fit by a single correlation (determined later). Typical number distributions for the data of this study are reported by Wang (1984). Figure 4 gives drop size distributions produced in the 0.15 m tank for the 0.1 Pa · s oil at various impeller speeds and at the two extremes of interfacial tension. Distributions are normal in volume and become broader as interfacial tension increases and impeller speed decreases.

The trend displayed in Figures 3 and 4 are common to most of the data. Except for the 1 Pa · s oil all distributions are normal in volume. The distribution broadens as μ_d and σ increase and as N decreases. According to Eq. 9, at constant D the relative resistance to breakage increases with μ_d and σ and decreases with N. As discussed in Part I, observations of breakage for low to moderate viscosity drops indicate a shift from bursting toward stretching as μ_d increases and as $Re(\sim NL^2)$ and D decrease. Furthermore, such a shift is consistent with a broadening of the distribution. A pattern emerges which suggests that E_R provides a measure of the broadness of the equilibrium distribution and the predominant breakage mode that determines it. The situation is actually more complicated, since the final distribution for a dilute, noncoalescing dispersion results from breakage of parents of many diameters. Not all drops break at the same location, so it is also determined by a spectrum of energy dissipation rates. Therefore at fixed conditions both D and R are variables in Eq. 9. It may be possible to characterize R by an average value for the impeller region. However, D is more difficult to characterize. For instance, a large drop has relatively low E_R and may burst violently into many smaller drops. If these are larger than the maximum stable diameter they will break again,

possibly by stretching; otherwise, they will remain stable. The final drop size distribution may be determined to some extent by the initial distribution or the method of introduction of the dispersed phase. This may only be important for large D_{32} (high σ and μ_d). In any event it appears that the broadness of the distribution and the predominant breakup mechanism determining it depend on system variables as given by Eq. 9.
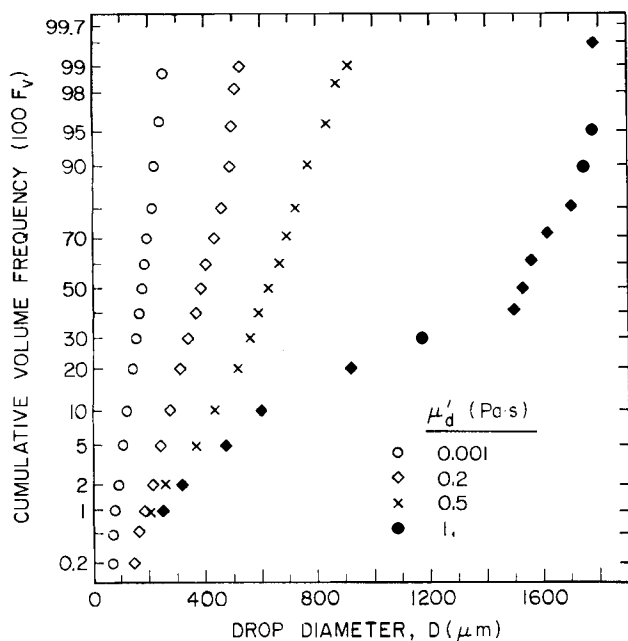
(a)
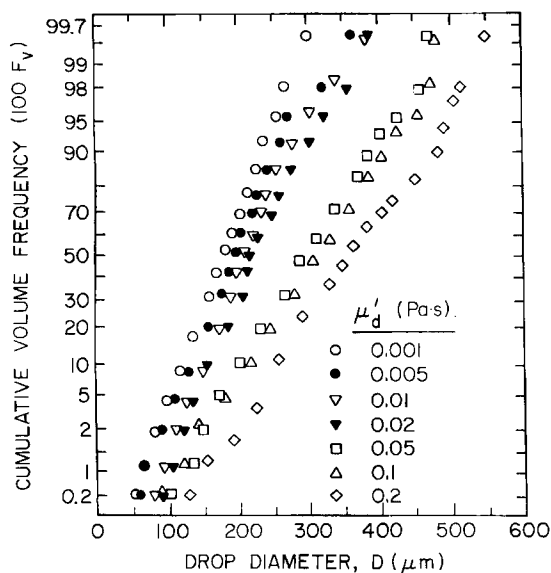
(b)

Figure 3. Effect of dispersed-phase viscosity on drop size distribution for silicone oils dispersed in water. $\sigma' = 0.045$ N/m; N = 4.67 rps; $T' = 0.15$ m.

(a) Lowest and higher viscosity grades.
(b) Middle viscosity grades.
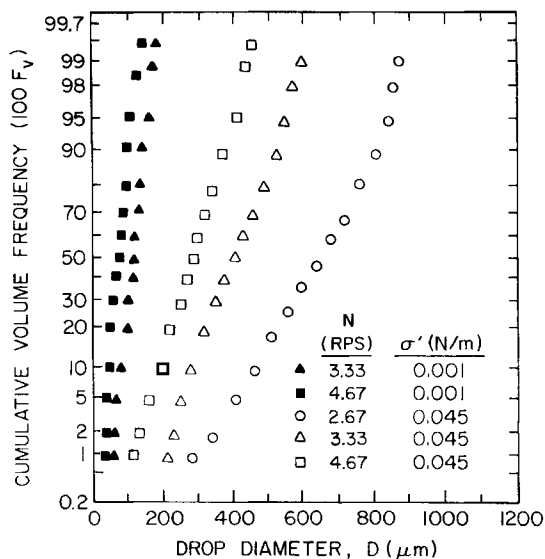
Figure 4. Effect of interfacial tension and impeller speed on drop size distribution. Data are for 0.1 Pa · s oil dispersed in water (open symbols) and in methanol (solid symbols). $\mu_d' = 0.1$ Pa · s; $T' = 0.15$ m.

Figure 5 reports data for the 1 Pa · s oil dispersed in various continuous phases in the 0.15 m tank at 4.67 rps. At low interfacial tension a normal distribution results. This occurred in all experiments where this oil was dispersed in methanol. At high σ considerable deviation from normality is seen. As in Part I, this occurred for all cases where this oil was dispersed in water. At moderate σ the distribution was often but not always normal. In Part I it was suggested that the functional form of the distribution is a measure of the ability of Eq. 1 to correlate mean size and of the predominant breakup mode. A transition region coincided with distributions that could not be characterized. If true,
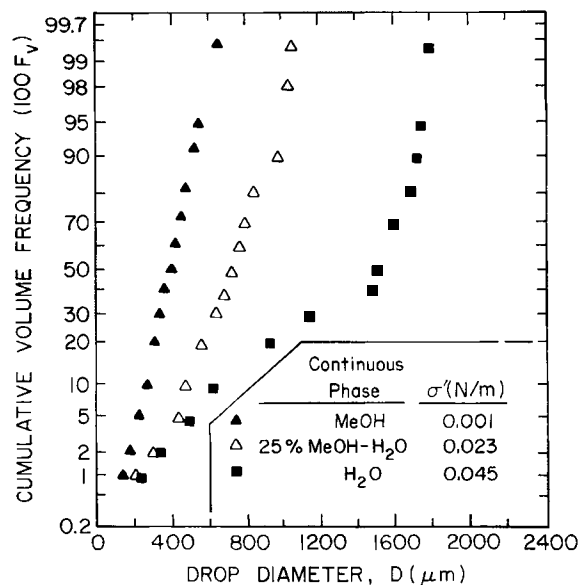

Figure 5. Effect of interfacial tension on functional form of drop size distribution for 1 Pa · s silicone oil. $\mu_d' = 1$ Pa · s; N = 4.67 rps; $T' = 0.15$ m.

then it appears that the transition does move to higher viscosity as σ decreases. Alternatively, a 1 Pa · s oil in a low σ system behaves as a moderate-viscosity oil. Since E_R (Eq. 9) increases with σ, the data of Figure 5 also suggest that E_R may be a measure of the transition between moderate- and high-viscosity behavior. Unfortunately, insufficient data were obtained to definitively characterize such a transition.

Mean Drop Size Correlations

Equation 1 and similar expressions were fitted to the low to moderate viscosity data via nonlinear least-squares regression to determine their suitability as correlations for Sauter mean diameter. The $\mu'_d = 1$ Pa · s data were excluded for reasons based on the previous discussion and the results of Part I. The semiempirical theory yielding Eq. 1 is capable of predicting the power to which We, Vi, etc. should be raised, but not geometric constants (A, B_1). To insure that the data were not being forced to these dependencies, the regression was run with an expression similar to Eq. 1 with powers unspecified. The result was

$$\frac{D_{32}}{L} = 0.066 \, We^{-0.66} \left[1 + 13.8 \, Vi^{0.82} \left(\frac{D_{32}}{L} \right)^{0.33} \right]^{0.59} \quad (12)$$

The goodness of fit of Eq. 12, shown in Figure 6, is excellent, as is expected for a six-parameter model. The root mean square deviation for the 146 data sets is $\sigma_{rms} = 9.6\%$, where

$$\sigma_{rms} = 100 \times \left[\frac{1}{n_D} \sum_{i=1}^{n_D} \left(\frac{D_{32E} - D_{32P}}{D_{32E}} \right)_i^2 \right]^{1/2} \quad (13)$$

Dependencies on We, Vi, etc. do not deviate substantially from those predicted by Eq. 1, lending credence to the semiempirical theory.

When fit to the same data, Eq. 1 yields

$$\frac{D_{32}}{L} = 0.054 \, We^{-3/5} \left[1 + 4.08 \, Vi \left(\frac{D_{32}}{L} \right)^{1/3} \right]^{3/5} \quad (14)$$

with $\sigma_{rms} = 21.1\%$. The goodness of fit of Eq. 14 is shown in Figure 7. At high D_{32}/L (large μ_d and σ) this correlation tends to underpredict the data. This may be due to the inability of the theory to account for the time required for breakup relative to the drop's residence time in the impeller region. The geometric constant $A = 0.054$ in Eq. 14 is essentially the same as the value $A = 0.053$ obtained by Chen and Middleman (1967) in using Eq. 3 to correlate their numerous low dispersed-phase viscosity data obtained under similar conditions.

A final correlation is that based on Eqs. 7 and 8. The result is

$$\frac{D_{32}}{L} = 0.053 \, We^{-3/5} [1 + 0.97 \, Vi^{0.79}]^{3/5} \quad (15)$$

where $\sigma_{rms} = 18.9\%$. A comparison of Figures 7 and 8 reveals that Eqs. 14 and 15 provide essentially the same fit to the data.

Based on goodness of fit, Eq. 12 is the preferred correlation. However, Eq. 15 is attractive due to its simplicity. Both indicate that the dependency of D_{32} on Vi is less than predicted by semi-theoretical arguments. For purposes of extrapolation, Eq. 14 should be used due to its mechanistic basis.
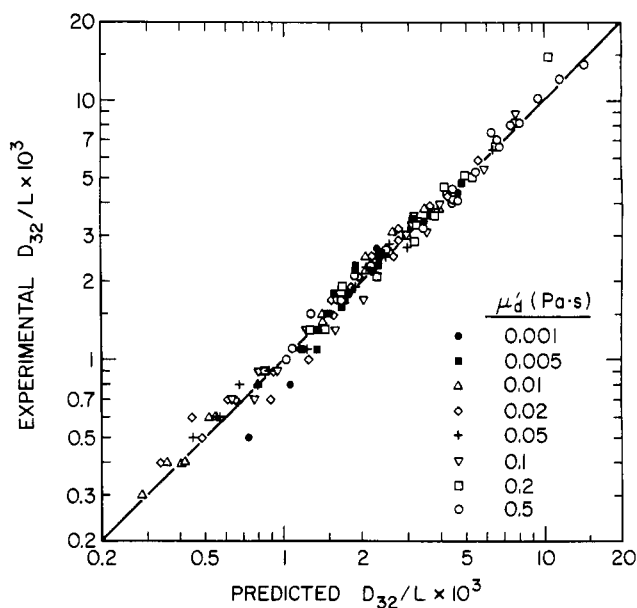

Figure 6. Goodness of fit of Eq. 12 to mean drop size data; $\sigma_{rms} = 9.6\%$.

An estimate of when dispersed-phase viscosity can be neglected is obtained from Eq. 6 using Eqs. 1 and 14. The result is

$$Vi \ll 0.65 \, We^{1/5} \quad (16)$$

For instance, consider $L = 0.15$ m, $N = 3$ rps, $\rho_c = \rho_d = 1,000$ kg/m³. For $\sigma = 0.01$ N/m, dispersed-phase viscous resistance to breakage is negligible for $\mu_d \ll 0.07$ Pa · s, say for $\mu_d < 0.007$ Pa · s. For $\sigma = 0.04$ N/m, viscous resistance can be ignored for μ_d's up to three times larger.

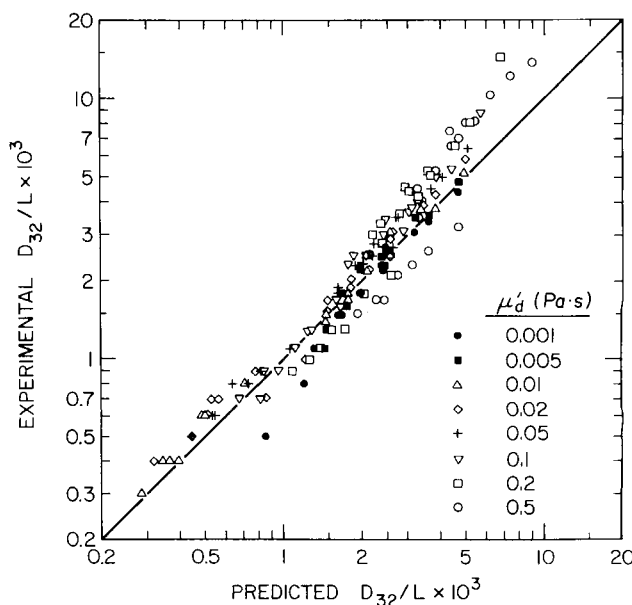The ratio of Sauter mean diameter to maximum stable drop

Figure 7. Goodness of fit of Eq. 14 to mean drop size data; $\sigma_{rms} = 21.1\%$.
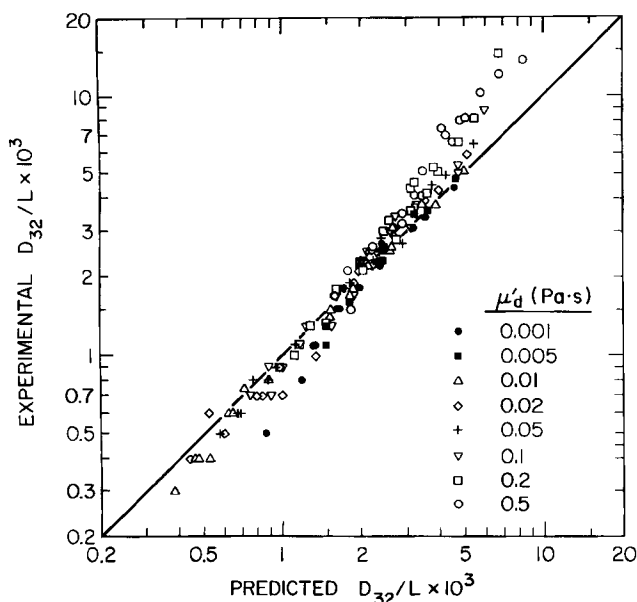
Figure 8. Goodness of fit of Eq. 15 to mean drop size data; $\sigma_{rms} = 18.9\%$.
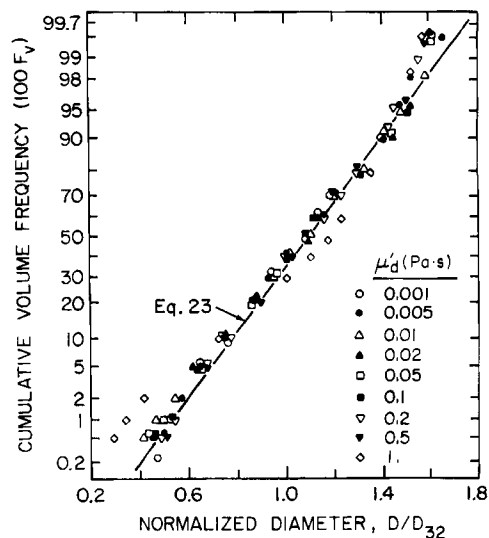

Figure 9. Similarity of normalized volume distribution for silicone oils dispersed in 25% MeOH-H$_2$O solution. $\sigma' = 0.023$ N/m; $N = 1.67$ rps; $T' = 0.3$ m.

size for all the data of this study is 0.61 ± 0.053. This is consistent with results reported in Part I for the same range of μ_d.

Correlation for Drop Size Distribution

Given that drop sizes are normally distributed in volume at low to moderate viscosity, it is desirable to correlate these by a single expression. Previous discussion with respect to Eq. 9 suggests that the probability density function, $P(D)$, which describes the equilibrium drop size distribution, may depend only upon E_R^{-1} (since E_R is inversely proportional to D); that is, $P(D) = \Omega(E_R^{-1})$. Such a conjecture is consistent with the approach of Chen and Middleman (1967) for low-viscosity dispersed phases ($E_v \simeq 0$). These authors assumed that $P(D) = \Omega(E_T/E_s)$, from which it followed that $P(D) = \Omega(D/D_{32P})$, where D_{32P} is the predicted value of D_{32} given by Eq. 3. They found that drop sizes were normally distributed in volume and could be correlated by normalization with D_{32}. Although the correlation failed in terms of D_{32P}, it was excellent when experimental Sauter mean diameters were used.

Equations 1 and 9 can be used to show that for finite Vi

$$P(D) = \Omega\left[\frac{D}{D_{32P}}; B_1 \, Vi\left(\frac{D_{32P}}{L}\right)^{1/3}\right] \qquad (17)$$

where D_{32P} is the value of D_{32} predicted by Eq. 1. The Chen and Middleman result is recovered as $Vi \rightarrow 0$. The form of the argument of Ω, although complicated, is such that in the limit $Vi \rightarrow \infty$, Eq. 17 reduces to $P(D) = \Omega(D/D_{32P})$ where D_{32P} is given by Eq. 4. It is evident from the results of Part I that Eq. 17 cannot be accommodated by a simple functional form, such as the normal distribution, over the entire range of Vi. This may be due to the violation of the principle of dynamic similarity (with respect to breakage mechanism) at high Vi. Given these concerns it is reasonable to adopt a more pragmatic approach. The Chen and Middleman experience casts doubt on any correlation involving predicted quantities such as D_{32P} and B_1. Since the

dependency of $P(D)$ on $B_1 \, Vi(D_{32P}/L)^{1/3}$ cannot be recast exclusively in terms of experimental variables, and since it vanishes for limiting cases, it is assumed, without proof, to be small. We therefore seek a correlation of the form $P(D) = \Omega(D/D_{32E})$ by inspection of the data.

Figures 9 to 11 show volume distributions, normalized with respect to experimental Sauter mean diameter, for a variety of conditions. These include variation, in turn, of dispersed-phase viscosity, interfacial tension, and impeller speed-tank size, with all other parameters held constant. Except for the 1 Pa · s oil of
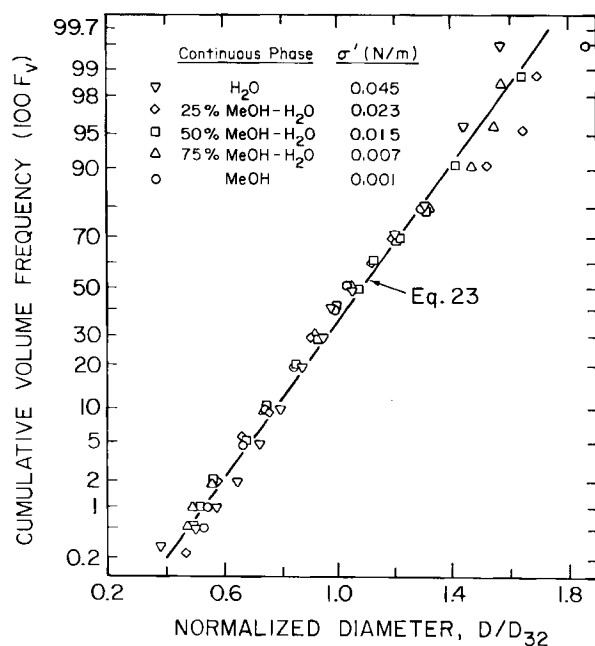

Figure 10. Similarity of normalized volume distribution for 0.02 Pa · s oil dispersed in various continuous phases. $\mu_d' = 0.02$ Pa · s; $N = 3.00$ rps; $T' = 0.2$ m.
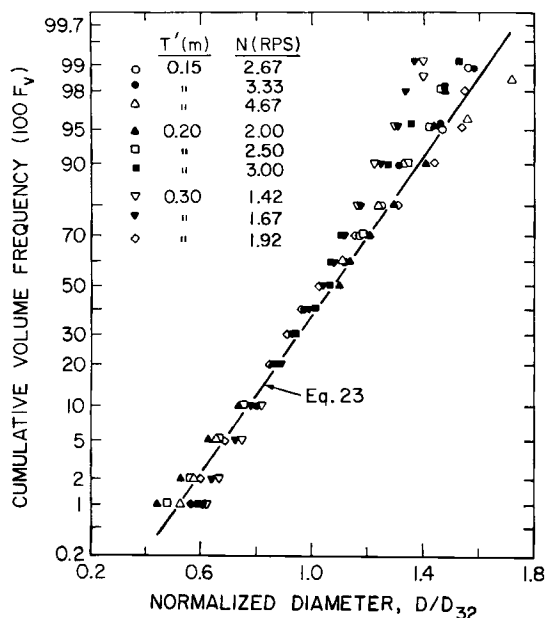
Figure 11. Similarity of normalized volume distribution for 0.05 Pa · s oil dispersed in water at various tank diameters and impeller speeds. $\mu_d' = 0.05$ Pa · s; $\sigma' = 0.045$ N/m.

Figure 9 and scatter in the tails of Figure 11, all data collapse approximately onto a straight line, indicating the feasibility of a single correlation for $\mu_d' \leq 0.5$ Pa · s. The solid lines in the figures represent the best-fit line for all of the data except $\mu_d' = 1$ Pa · s, as discussed subsequently.

The following model for the probability density function with respect to volume was used to fit the data. For a normal distribution ($X = D/D_{32}$):

$$P_v(X) = \frac{1}{\sqrt{2\pi}\,\sigma_v} \exp\left[-\frac{(X - \overline{X})^2}{2\sigma_v^2}\right] \qquad (18)$$

where

$$\overline{X} = \sum_{i=1}^{n_T} D_i^3 X_i \Bigg/ \sum_{i=1}^{n_T} D_i^3 \qquad (19)$$

$$\sigma_v^2 = \sum_{i=1}^{n_T} D_i^3 (X_i - \overline{X})^2 \Bigg/ \sum_{i=1}^{n_T} D_i^3 \qquad (20)$$

The cumulative volume frequency is given by

$$F_v(X) = \int_{-\infty}^{x} P_v(X')dX' \qquad (21)$$

Substituting Eq. 18 into Eq. 21 yields

$$F_v(X) = 0.5\left[1 + \text{erf}\left(\frac{X - \overline{X}}{\sqrt{2}\,\sigma_v}\right)\right] \qquad (22)$$
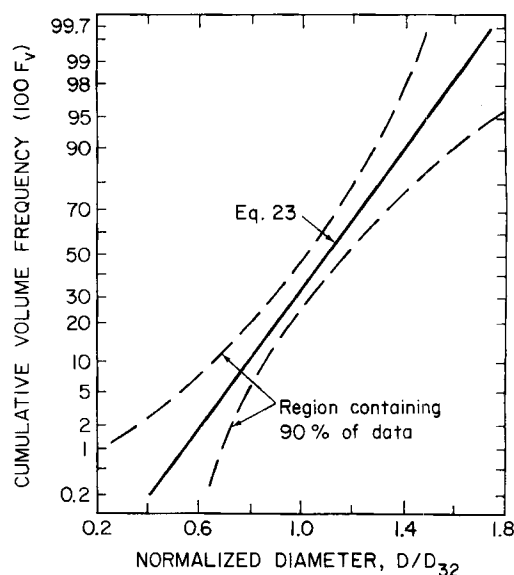

Figure 12. Goodness of fit of Eq. 23 to drop size distribution data. – – – encloses region containing 90% of the data.

Equation 22 was fitted to the 146 data sets for $\mu_d' \leq 0.5$ Pa · s via nonlinear least-squares regression. At least fifteen values of $F_v(X)$ were used to describe each individual distribution. The $\mu_d' = 1$ Pa · s data were excluded for reasons discussed previously. The result is

$$F_v(D/D_{32}) = 0.5\left[1 + \text{erf}\left(\frac{D/D_{32} - 1.07}{0.24\,\sqrt{2}}\right)\right] \qquad (23)$$

The fraction of total volume contained by drops of size D to $D + dD$ is given by

$$f_v(D, D + dD) = F_v\left(\frac{D + dD}{D_{32}}\right) - F_v(D/D_{32}) \qquad (24)$$

Figure 12 shows Eq. 23 bounded by the region containing 90% of the data. The broadening of this region at low and high D/D_{32} is mostly due to scatter in the tails of the individual distributions and not to significant changes in the slopes of the individual curves. There was no evidence to indicate that a better correlation could be obtained by considering only lower values of viscosity and/or interfacial tension.

Equation 23 can be compared with the correlation obtained by Chen and Middleman for their 110 low viscosity data sets:

$$F_v(D/D_{32}) = 0.5\left[1 + \text{erf}\left(\frac{D/D_{32} - 1.06}{0.23\,\sqrt{2}}\right)\right] \qquad (25)$$

Equations 23 and 25 are virtually indistinguishable, indicating that normalized drop size distributions, for dilute suspensions produced in tanks of standard geometry equipped with six-blade Rushton turbines, do not differ for low to moderate viscosity dispersed phases.

Acknowledgment

Notation

A = dimensionless empirical constant, Eqs. 1, 3, 4, 6, and 7
B_1 = dimensionless empirical constant, Eqs. 1, 4, and 6
B_2 = dimensionless empirical constant, Eq. 8
c = dimensionless empirical constant, Eq. 8
D = diameter of drop
D_{32} = Sauter mean diameter
D_{32E} = experimental value of D_{32}
D_{32P} = predicted value of D_{32}
E_R = relative resistance to breakage, Eq. 9
E_s = surface energy of drop
E_T = turbulent energy available to disrupt drop
E_v = viscous energy of drop
F_v = cumulative volume frequency
$f_v(D, D + dD)$ = fraction of total volume contained in drops of size D to $D + dD$
L = impeller diameter
N = impeller speed
$N_{Vi} = (\rho_c/\rho_d)^{1/2} \mu_d \bar{\epsilon}^{1/3} D_{32}^{1/3}/\sigma$; viscosity group proposed in Part I
$N'_{Vi} = \mu_d/\sqrt{\rho_d \sigma D}$; viscosity group proposed by Hinze (1955)
n_D = number of data points used in regression analysis
n_T = total number of drop counts
$P(D)$ = probability density function for equilibrium drop size distribution
$P_v(X)$ = probability density function, Eq. 18
$R = \epsilon/\bar{\epsilon}$; ratio of local to mean energy dissipation rate
Re = tank Reynolds number, Eq. 5
T' = nominal tank diameter
Vi = tank viscosity group, Eq. 2b
We = tank Weber number, Eq. 2a
$X = D/D_{32}$; normalized drop diameter
$\bar{X}$ = mean of X, Eq. 19

Greek letters

α_1, α_2 = empirical constants, Eq. 9
ϵ = local energy dissipation rate per unit mass
$\bar{\epsilon}$ = average power input per unit mass or mean energy dissipation rate per unit mass
$\Omega(Y)$ = unknown function of Y
μ_c = viscosity of continous phase
μ_d = viscosity of dispersed phase
μ'_d = nominal dispersed-phase viscosity
ρ_c = density of continuous phase
ρ_d = density of dispersed phase
σ = interfacial tension
σ' = nominal interfacial tension
σ_{rms} = root mean square deviation, Eq. 13
σ_v = standard deviation of drop size, Eq. 20
ϕ = volume fraction of dispersed phase
$\psi(Z)$ = unknown function of Z

Literature Cited

Brown, D. E., and K. Pitt, "Drop Breakup in a Stirred Liquid-Liquid Contactor," *Proc. Chemeca 70*, Melbourne and Sydney, 83 (1970).

Chen, H. T., and S. Middleman, "Drop Size Distribution in Agitated Liquid-Liquid Systems," *AIChE J.*, **13**, 989 (1967).

Hinze, J. O., "Fundamentals of the Hydrodynamic Mechanism of Splitting in Dispersion Processes," *AIChE J.*, **1**, 289 (1955).

Narsimhan, G., J. P. Gupta, and D. Ramkrishna, "A Model for Transitional Breakage Probability of Droplets in Agitated Lean Liquid-Liquid Dispersions," *Chem. Eng. Sci.*, **34**, 257 (1979).

Sleicher, C. A., Jr., "Maximum Stable Drop Size in Turbulent Flow," *AIChE J.*, **8**, 471 (1962).

Tavlarides, L. L., and M. Stamatoudis, "The Analysis of Interphase Reactions and Mass Transfer in Liquid-Liquid Dispersions," *Adv. Chem. Eng.*, **11**, 199 (1981).

Wang, C. Y., "The Effect of Dispersed-Phase Viscosity on Mean Drop Sizes and Drop Size Distributions in Turbulent Stirred-Tank Contactors," Ph.D. Thesis, Univ. Maryland (1984).